Response Properties of Saccade-Related Burst Neurons in the Central Mesencephalic Reticular Formation

ARI HANDEL AND PAUL W. GLIMCHER
Center for Neural Science, New York University, New York, New York 10003

Handel, Ari and Paul W. Glimcher. Response properties of saccade-related burst neurons in the central mesencephalic reticular formation. *J. Neurophysiol.* 78: 2164–2175, 1997. We studied the activity of saccade-related burst neurons in the central mesencephalic reticular formation (cMRF) in awake behaving monkeys. In *experiment 1,* we examined the activity of single neurons while monkeys performed an average of 225 delayed saccade trials that evoked gaze shifts having horizontal and vertical amplitudes between 2 and 20°. All neurons studied generated high-frequency bursts of activity during some of these saccades. For each neuron, the duration and frequency of these bursts of activity reached maximal values when the monkey made movements within a restricted range of horizontal and vertical amplitudes. The onset of the movement followed the onset of the burst by the longest intervals for movements within a restricted range of horizontal and vertical amplitudes. The range of movements for which this interval was longest varied from neuron to neuron. Across the population, these ranges included nearly all contraversive saccades with horizontal and vertical amplitudes between 2 and 20°. In *experiment 2,* we used the following task to examine the low-frequency prelude of activity that cMRF neurons generate before bursting: the monkey was required to fixate a light-emitting diode (LED) while two eccentric visual stimuli were presented. After a delay, the color of the fixation LED was changed, identifying one of the two eccentric stimuli as the saccadic target. After a final unpredictable delay, the fixation LED was extinguished and the monkey was reinforced for redirecting gaze to the identified saccadic target. Some cMRF neurons fired at a low frequency during the interval after the fixation LED changed color but before it was extinguished. For many neurons, the firing rate during this interval was related to the metrics of the movement the monkey made at the end of the trial and, to a lesser degree, to the location of the eccentric stimulus to which a movement was not directed.

INTRODUCTION

The highly stereotyped trajectories of saccadic eye movements are produced by temporally patterned activations of oculomotoneurons (Fuchs and Luschei 1970; Robinson 1970). Several lines of evidence suggest that *1*) brain stem and mesencephalic medium lead burst neurons (MLBNs) participate in the generation of this activity (for reviews, see Fuchs et al. 1985; Moschovakis and Highstein 1994; Sparks and Mays 1990) and *2*) these brain stem neurons are activated, either directly or indirectly, by saccade-related burst neurons (SRBNs) in the superior colliculus (SC) and frontal eye fields (Chimoto et al. 1996; Fuchs et al. 1985; Raybourn and Keller 1977; Sparks and Mays 1990). In this report we present a characterization of the response properties of SRBNs in the central mesencephalic reticular formation (cMRF). cMRF neurons that have been proposed to play a role in the transmission of movement-related signals from the SC to MLBNs (Moschovakis and Highstein 1994; Sparks and Mays 1990; Waitzman et al. 1996).

SRBNs in the cMRF, like some neurons in the SC (Glimcher and Sparks 1992; Sparks 1978; Wurtz and Goldberg 1972), have been reported to generate both an occasional low-frequency prelude of activity and a high-frequency saccade-related burst of activity (Waitzman 1982). The number of spikes in the burst of most of these neurons has been reported to be larger for contralateral movements than for ipsilateral movements, although these data indicated that the activity of many neurons was also dependent on vertical saccadic amplitude (Waitzman et al. 1996). For some cMRF neurons, burst offset was reported to coincide with movement offset (Waitzman et al. 1996). Largely on the basis of these observations and the finding by Cohen et al. (1985) that microstimulation of the cMRF region produced purely contraversive movements, cMRF neurons have been proposed to play a role in *1*) providing horizontally tuned pontine MLBNs with a signal encoding the horizontal component of the movement vector specified by bursts of activity in the population of collicular SRBNs (Sparks and Mays 1990; Waitzman et al. 1996) and/or *2*) providing the SC with efferent signals from the pontine MLBNs for use in the dynamic control of movements (Waitzman et al. 1996).

Thus cMRF burst neurons have been hypothesized to participate, together with MLBNs, in the execution of movements initiated by the SC (Waitzman et al. 1996). In the present study we have used three methods to investigate whether the response properties of cMRF SRBNs are commensurate with this hypothesis. First, we examined the spatial tuning of cMRF neurons to determine whether information about movement metrics can be extracted from the identity of the active population of neurons, the firing rate of individual neurons, or a combination of both. Second, we examined the temporal relation between burst onset in cMRF neurons and movement onset to estimate when information about saccade onset time is first present in the population. Finally, we examined the response of cMRF neurons during tasks designed to reveal signals appropriate for movement-related processes that precede the neural command to initiate a saccade.

METHODS

General methods

Two juvenile male rhesus macaques (*Macaca mulatta*) were employed as subjects in the following experiments. All animal procedures were designed in conjunction with the University Veter-

inarian, were approved by the New York University Institutional Animal Care and Use Committee, and were conducted in compliance with the Public Health Service's Guide for the Care and Use of Animals.

Two surgical procedures were conducted on each monkey under sterile conditions and isoflurane/nitrous oxide anesthesia. Postsurgically, animals received analgesics and antibiotics for a minimum of 3 days. In the first procedure we implanted a scleral search coil (Fuchs and Robinson 1966; Judge et al. 1980) in one eye and mounted a head restraint prosthesis to the skull with the use of standard orthopedic techniques. After recovering from the first surgery, monkeys were allowed only restricted access to water in their home cages and were trained to perform the behavioral tasks used in this study for a fruit juice reward provided on a VR3 reinforcement schedule (on average, 1 reward for every 3 correct trials). A 300-ms noise burst served as a secondary reinforcer on all correct trials. When training was complete, in a second sterile surgical procedure a 15-mm craniotomy was made and a stainless steel cylinder was mounted on the skull above it (coordinates: 7.5 mm anterior and 4.5 mm lateral to the intraaural point).

With the use of the search coil technique (Fuchs and Robinson 1966), the horizontal and vertical direction of gaze could be determined with a sensitivity of $>0.25°$ of arc and was sampled at 500 Hz. At the beginning of each experimental session a tungsten steel electrode (1.0–10.0 MΩ, Frederick Haer) was withdrawn into a sharpened 23-gauge hypodermic tube (0.064 mm OD) that was used to pierce the dura and to serve as a guide tube. A hydraulic microdrive was then used to advance the electrode into the brain. Initially, penetrations were made medially in the cylinder until single-unit response properties and stimulation-evoked eye movements indicated that the electrode tip was located in the oculomotor nucleus (Schiller 1970). On successive penetrations, the guide tube was moved laterally in 1-mm steps until saccade-related neurons were encountered at approximately the same depth as the oculomotor nucleus. At that point, the systematic search for units with the properties of cMRF SRBNs was begun. The waveforms of individual neurons were isolated using time and amplitude criteria. The time of occurrence of individual spikes was recorded by computer with 1-μs precision.

Monkeys were trained to make saccadic eye movements in response to the onset and offset of tri-state light-emitting diodes (LEDs) that could be illuminated to appear red, green, or yellow to normal human observers. These LEDs were spaced in 2-in. intervals on a planar screen placed 57 in. from the eyes of the animal. Four hundred forty-one of these LEDs spanned 40° of horizontal and 40° of vertical visual angle.[1]

Experiment 1: characteristics of saccade-related bursts of activity

Experiment 1 was designed to determine the precise spatial and temporal tuning of the perimovement burst of action potentials produced by cMRF SRBNs. When a cell with saccade-related increases in firing rate was encountered, we presented the monkey with 10–50 delayed saccade trials. A delayed saccade trial (Fig. 1*A*) began with the illumination of a central yellow LED with which the monkey had 1,000 ms to align gaze (±3°). After a 200- to 800-ms delay, an eccentric yellow LED was illuminated while the animal was required to maintain fixation of the central LED. After a further 400- to 1,200-ms delay, the central LED was extinguished, cuing the animal that a saccade that shifted gaze into alignment with the eccentric LED (±4°) within 350 ms would be reinforced. During this initial set of trials, the eccentric targets to which the animals were required to direct gaze were located randomly on the tangent screen. To ensure that no neurons from the oculomotor nucleus were included in the population of neurons we sampled, only neurons for which the number of action potentials produced 50–25 ms before the onset of the saccade varied as a systematic function of movement metrics were investigated further.[2] We recorded the responses of 25 neurons that met these criteria while the animal completed a minimum of 75 delayed saccade trials (mean = 225 trials, maximum = 577 trials). On each of these trials, the position of the eccentric target was randomly chosen from any of the locations on the tangent screen. For a subset of neurons that responded maximally for small amplitude movements, we preferentially sampled the central 6° of the tangent screen. For these trials, the criterion for gaze alignment with the fixation LED was ±1° and the criterion for gaze alignment with the eccentric target location was ±1–2°.

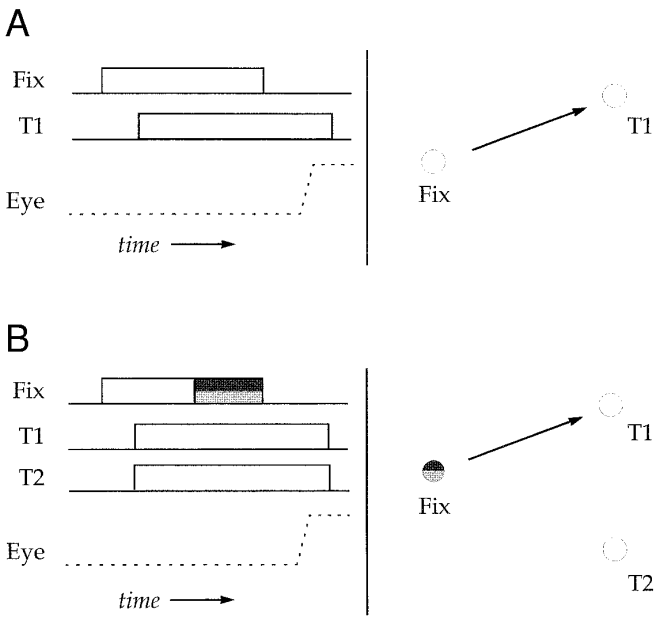

FIG. 1. Sequence of events for each task is presented at *left;* spatial relationship between representative light-emitting diodes (LEDs) is presented at *right. A*: delayed saccade task. Trials began with illumination of central yellow LED (Fix) with which monkey had 1,000 ms to align gaze (±3°). After a 200- to 800-ms interval, an eccentric yellow LED (T1) was illuminated. After a further 400- to 1,200-ms delay, central LED was extinguished, cuing animal that saccade that shifted gaze into alignment with T1 (±4°) within 350 ms would be reinforced. *B*: cued saccade task. These trials began with illumination of central yellow LED (Fix) with which monkey had 1,000 ms to align gaze (±3°). After delay of 200–800 ms, 2 eccentric LEDs were illuminated yellow, 1 above fixation (T1) and 1 below it (T2). After an additional 400- to 1,200-ms delay, color of central LED changed to either red or green. Switch to red specified that saccadic goal would be T1, whereas switch to green specified that it would be T2. Monkey was required to maintain fixation of central LED for an additional 200–800 ms, until it was extinguished, cuing animal that saccade that shifted gaze into alignment (±4°) with saccadic goal (T1 or T2) within 350 ms would be reinforced.

ANALYSIS. After an experimental session was complete, the data were subjected to a two-stage analysis. In the first stage of analysis the amplitude, direction, and onset and offset times of each trial-associated movement were determined. Movement onset was de-

[1] Throughout this paper the locations of LEDs are reported without correction for the tangent error, never $>0.7°$, induced by the planar stimulus display. All numerical calculations, however, are based on corrected LED locations.

[2] In principle, this methodology would exclude neurons that generated eye-movement-related modulations in firing rate only ≤25 ms before saccades. In practice, ~2 neurons having this type of response were encountered in the penetrations that yielded the neurons presented here.

fined as the time at which the horizontal or vertical component of eye velocity exceeded 40°/s; however, the distribution of movement onset times for a typical data set (as illustrated in Fig. 3*A*) did not differ substantially when movements were detected with either a velocity criterion of 40°/s (saccadic latency = 241 ± 30 ms, mean ± SD) or with a velocity criterion of 10°/s (saccadic latency = 237 ± 28 ms, mean ± SD). We also determined the onset time, offset time, and number of spikes within any high-frequency burst that followed the offset of the fixation point with the use of the following algorithm: for each neuron, the mean firing rate, during a 25-ms interval ending at the offset of the fixation light, was measured and the mean and SD of this rate across all delayed saccade trials for that neuron was calculated. A burst was defined as a series of five or more consecutive spikes with instantaneous frequencies ≥4 SD above this mean. Burst onset was defined as the time of occurrence of the first spike in this group and burst offset was defined as the time of occurrence of the last spike in this group. Mean firing rate during a burst was defined as the total number of spikes in the burst divided by burst duration. Burst lead was defined as the time of movement onset minus the time of burst onset.

Once the data base for each neuron was compiled, we were able to examine burst parameters as a function of movement metrics for all of the movements in a data set. Specifically, for each neuron we generated three-dimensional graphs (movement fields) of *1*) burst duration, *2*) mean firing rate during the burst, and *3*) burst lead as a function of the horizontal and vertical amplitude of the movement produced at the end of each reinforced trial.

Burst lead was analyzed further: the center of the burst lead movement field was defined as the smallest convex polygon that would enclose the movements from all the trials for which burst lead was ≥80% of the maximum burst lead observed for that neuron. For the purposes of this analysis, we included only trials in which the burst lead was within 0.2 log units of the burst lead on at least three other trials. This method excluded, on average, one outlier trial, showing an extremely large burst lead, from each neuronal data set. Note that although these polygons enclosed all the movements associated with the longest burst leads generated by a neuron, they did not necessarily enclose only those movements.

Experiment 2: characteristics of pre-burst activity

Experiment 2 was designed to characterize signals carried in the low-frequency activity that many cMRF neurons have been reported to generate before their high-frequency bursting activity. Twenty-six neurons meeting our criteria for identification of cMRF SRBNs were studied in *experiment 2* (10 of these neurons were also included in *experiment 1*) with a minimum of 100 cued saccade trials (mean = 343 trials, maximum = 840 trials). Once a neuron had been isolated and examined for saccade-associated discharges we used the delayed saccade task to identify a range of movements for which the activity of the neuron was unmodulated. Monkeys were then presented with a series of cued saccade trials. A cued saccade trial (Fig. 1*B*) began with the illumination of a central yellow LED with which the monkey had 1,000 ms to align gaze (±3°). After a delay of 200–800 ms, two eccentric LEDs were illuminated yellow, one above and one below the central LED. After an additional 400- to 1,200-ms delay, the color of the central LED changed to either red or green. A switch to red specified that the saccadic target would be the upper eccentric LED, whereas a switch to green specified that the lower LED would serve as the saccadic target. The monkey was required to maintain fixation of the red or green central LED for an additional unpredictable interval of 200–800 ms. The central LED was then extinguished, cuing the animal that a saccade that shifted gaze into alignment with the saccadic target (±4°) within 350 ms would be reinforced.

During these cued saccade trials the location of one of the eccentric LEDs was always fixed at a location associated with no modulations of activity during the delayed task. The position of the second eccentric LED was varied randomly, from trial to trial, within the hemifield (upper or lower) in which the fixed stimulus was not located. In this way, modulations of neuronal activity on a given cued saccade trial could be attributed primarily to the location of the variably placed eccentric LED. Because this LED served as a target on one half of all trials and as a distractor on the other half, we were able to examine the responses of the neuron as a function of both the spatial position of the irrelevant distractor and the metrics of the target-guided saccades.

ANALYSIS. For each cued saccade trial, the number of action potentials produced by the neuron during three intervals was determined. These intervals were *1*) the visual interval, a 200-ms interval beginning at the onset of the eccentric LEDs; *2*) the cue interval, a 200-ms interval ending at the unpredictable offset of the fixation stimulus; and *3*) the movement interval, a 100-ms interval beginning 50 ms before saccade onset.

Reinforced cued saccade trials were then sorted into two groups for analysis: those on which the variably located eccentric LED served as the saccadic target (target trials), and those on which the variably located eccentric LED served as an irrelevant distractor (distractor trials). We analyzed the activity associated with target trials by generating three three-dimensional plots for each neuron. These three-dimensional graphs presented the firing rate of the neuron during the visual, cue, and movement intervals as a function of the amplitude and direction of the movement at the end of the trial. We analyzed distractor trials by generating three similar plots that presented firing rate during the visual, cue, and movement intervals as a function of the horizontal and vertical position of the irrelevant distractor. We were thus able to generate pairs of plots for each interval from which it was possible to compare the activity of the neuron on trials in which a particular LED served as a saccadic goal versus trials in which that same LED served as an irrelevant distractor.

To quantify the magnitude of the difference between the maximal activity a neuron produced on trials when the variable LED served as a target and on trails when the variable LED served as a distractor, we computed a selectivity ratio for each neuron, during each interval, in the following manner: first, the data that made up each three-dimensional plot were averaged in logarithmically scaled polar coordinate bins (45° in width and 0.2 log deg in amplitude). The maximally valued bins were then identified in both the target and distractor plots. A contrast ratio for selectivity during each interval was then computed as (MaxTarget − MaxDistractor)/(MaxTarget + MaxDistractor). This ratio can, in principle, range from −1 to +1, where +1 indicates that a neuron is completely unresponsive to LEDs that serve as distractors, −1 indicates that a neuron is unresponsive to LEDs that serve as targets, and 0 indicates that a neuron is equally responsive to an LED regardless of its role in the task.

Histological analysis

In the final weeks of these experiments, additional neurons from one animal were examined with the use of the preceding experimental protocols. After each of these neurons was studied, an electrolytic lesion was placed at the recording site by passing a 5-μA cathodal current through the recording electrode for 5 s. The animal in which these lesions had been placed was then preanesthetized with ketamine and killed by a lethal intravenous overdose of thiopental sodium. The animal was then perfused transcardially with a balanced salt solution, followed by 4% paraformaldehyde in phosphate-buffered saline, followed by 30% sucrose in phosphate-buffered saline. The brain was removed from the skull and placed in 4% paraformaldehyde/30% sucrose for 2 wk. The

tissue was blocked and cut on a freezing microtome in 40-μm sections. Sections were mounted and stained with Thionine. Camera lucida reconstructions of all lesion sites were made for analysis.

RESULTS

Experiment 1: saccade-related bursts of cMRF neurons

SINGLE-TRIAL DATA. Figure 2 plots the activity of a representative neuron during six delayed saccade trials in which gaze was shifted from fixation to different locations. *A–F* plot the horizontal and vertical position of the eye and the instantaneous firing frequency of the neuron as a function of time during a 600-ms interval centered on movement onset; the arrows indicate the time of the offset of the fixation LED. The numbers in parentheses above each panel identify the Cartesian coordinates of the eccentric LED that served as the target of the saccade, in degrees of visual angle with reference to the fixation LED. Bursts of action potentials, as defined by our algorithm (see METHODS), are shaded gray.

Figure 2*C* depicts a delayed saccade trial during which the monkey made a saccade that shifted gaze within ±4° of a target located 20° downward and 20° to the left (contralateral) of the fixation LED. On this trial, the neuron fired at a low frequency for hundreds of milliseconds, beginning before the cue to move, and then generated a high-frequency burst that began 88 ms before the movement, lasted for 188 ms, and whose mean firing rate was 138 Hz. For this neuron, bursts typically had lower mean frequencies, shorter durations, and began in closer temporal proximity to movement onset (shorter burst leads) on trials where saccades had smaller downward and/or contraversive components. However, for this neuron the temporal relationship between the offset of the burst and the offset of the movement was relatively constant across trials. Note that during a trial when the monkey made a saccade that shifted gaze within ±4° of a target located 4° upward and 20° contralateral to the point of fixation, the neuron did not generate a high-frequency burst of activity (Fig. 2*A*).

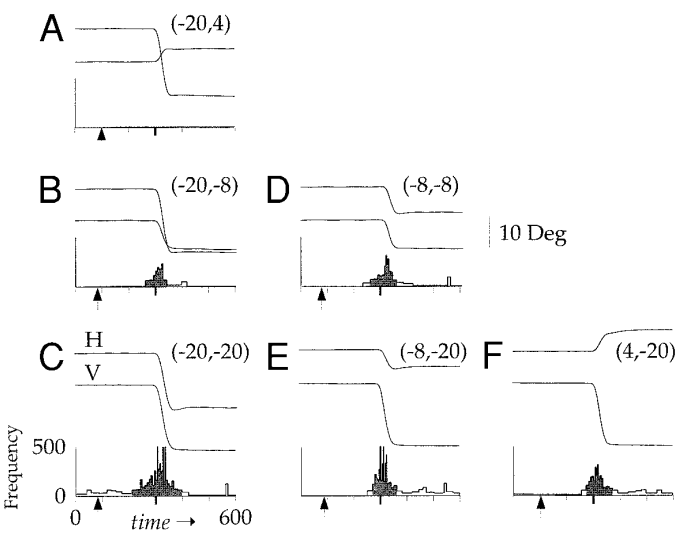

FIG. 2. Activity of single unit plotted for single delayed saccade trials on which both target position and saccade metrics varied systematically. Horizontal and vertical eye position are plotted as function of time above histogram of instantaneous firing frequency of neuron. Bursts, as detected by our algorithm, are shaded gray. Arrows: time of fixation offset. Horizontal and vertical coordinates of eccentric target LED, in deg of visual angle, are presented in parentheses above each eye position trace. Mean burst frequencies (in Hz): 0 (*A*), 113 (*B*), 138 (*C*), 120 (*D*), 174 (*E*), and 140 (*F*). Burst durations (in ms): 0 (*A*), 80 (*B*), 188 (*C*), 100 (*D*), 92 (*E*), and 100 (*F*). Burst leads (in ms): 0 (*A*), 40 (*B*), 88 (*C*), 50 (*D*), 22 (*E*), and 26 (*F*).

SPATIAL TUNING OF BURST PARAMETERS. For each neuron, the possibility that some burst parameters varied systematically with saccade metrics was examined by plotting, for all reinforced delayed saccade trials, *1*) mean burst firing rate, *2*) burst duration, and *3*) burst lead (the interval between burst onset and movement onset) as a function of the horizontal and vertical amplitude of the saccade. Figure 3 shows these three plots for each of three representative neurons. In each plot, the color of each square represents the average value for all movements with horizontal and vertical amplitudes corresponding to that pixel.

Note that all three burst parameters varied systematically with the metrics of the accompanying movement. For the neuron illustrated in Fig. 3*A* (representative single trials are shown in Fig. 2), which was most active for large amplitude downward and contraversive movements, the breadth of the spatial tuning appears to have been roughly equivalent for all three burst parameters. The neuron illustrated in Fig. 3*B*, which responded most vigorously for ipsilateral and downward movements, showed relatively broader spatial tuning across all three burst parameters. For this neuron the tuning of burst duration appeared to be narrowest, whereas the tuning for mean rate appeared broadest. Finally, the neuron illustrated in Fig. 3*C*, which was most active for upward and contraversive movements, showed relatively narrow spatial tuning across all three burst parameters, although the tuning of mean firing frequency and burst duration appeared broader than the tuning for burst lead.

Across all trials on which a burst was generated, we computed pair-wise correlation coefficients (r) between burst parameters on a trial-by-trial basis. Although the spatial tuning of all three burst parameters appeared similar, as illustrated in Fig. 3, trial-by-trial correlations were low. The mean r^2 between burst duration and burst lead (0.302 ± 0.050, mean ± SE) was larger than the mean r^2 between mean frequency and burst lead (0.069 ± 0.015, mean ± SE) and the mean r^2 between mean frequency and burst duration (0.062 ± 0.017, mean ± SE).

TEMPORAL CORRELATIONS: BURST ONSET AND SACCADE ONSET. Although all the neurons we studied appeared to show some degree of spatial tuning when burst lead was plotted as a function of horizontal and vertical movement amplitude, the overall breadth of tuning and the range of movements associated with the longest lead bursts appeared to vary from neuron to neuron. We chose to represent the spatial extent of burst lead tuning, and thus to define a movement field center, by plotting, for each neuron, the smallest convex polygon that enclosed the movements from all trials in which the burst lead was ≥80% of the maximum burst lead for that neuron. We chose this representation because it does not rely on a specific geometric model of the neuronal spatial tuning function. However, it should be noted that whenever an edge of the polygon fell near the edges of our sampling

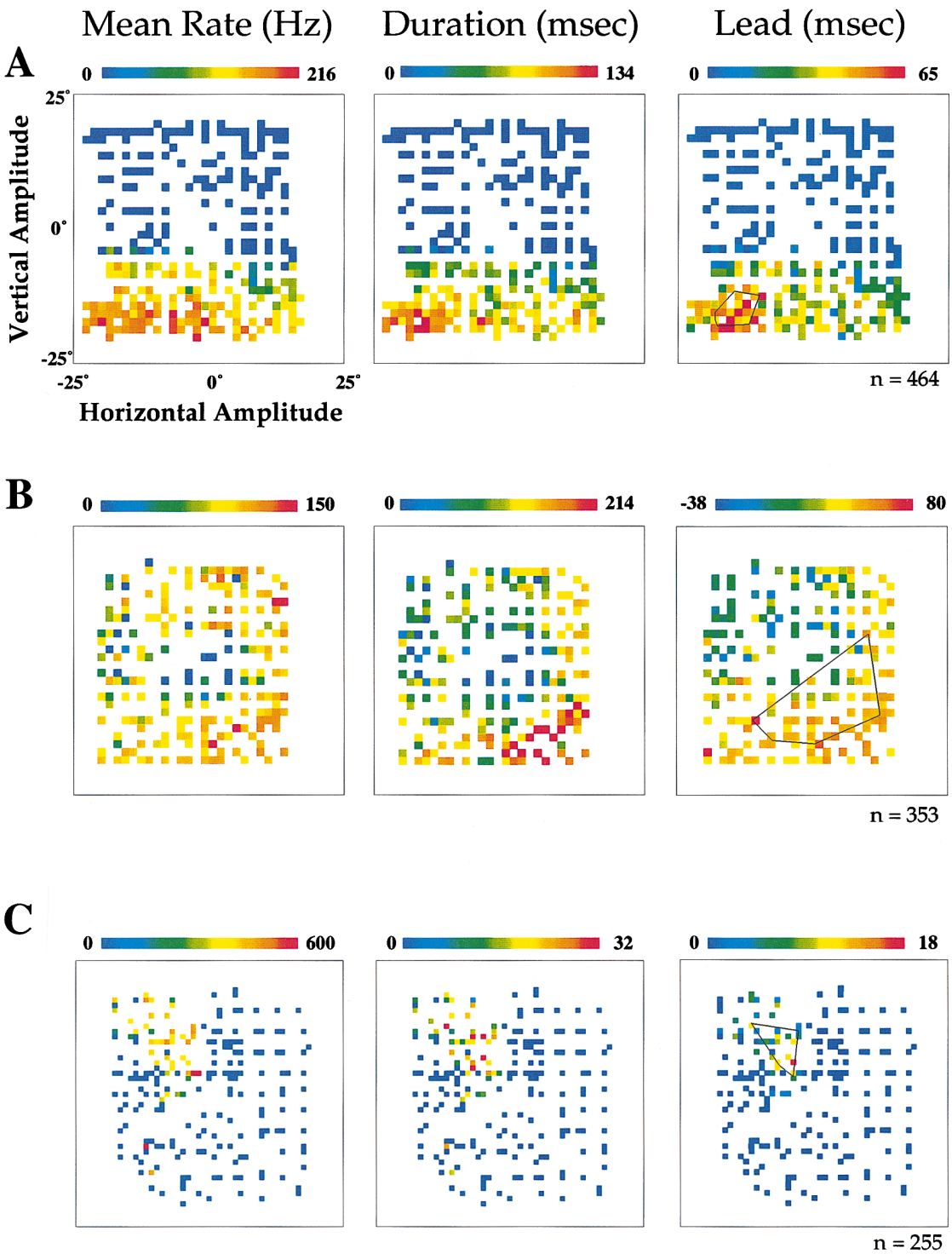

FIG. 3. Mean frequency, duration, and lead of burst during all reinforced delayed saccade trials plotted as function of horizontal and vertical amplitude of movement for 3 neurons from right central mesencephalic reticular formation (cMRF; *neurons p070795, p0720952,* and *s012596,* respectively). In *A* and *B,* data were averaged in 2 × 2° bins; in *C* 1 × 1° bins were used. Mean value of burst parameter associated with each bin is represented by its color, according to scale above each plot. If no burst was detected, then burst duration, mean firing rate during burst, and burst lead were arbitrarily assigned a value of 0. Superimposed on each burst lead plot is polygon enclosing movements from trials on which burst lead was within 80% of maximal burst lead observed for that neuron.

range, the outer boundaries of that polygon were likely to reflect the boundaries of our sample space.

These polygonal representations of the burst lead spatial tuning (movement field centers) are presented in Fig. 3, overlaid on the burst lead plots (Fig. 3, *right*). Note that the polygons capture both the range of movements that elicited

the longest lead bursts and the relative breadth of burst lead tuning for these neurons. On average, 38 ± 21% (SD) of all movements into the movement field centers of the neurons we sampled were associated with bursts whose onset led movement onset by ≥80% of the maximal burst lead.

Figure 4 plots, on a single graph, the polygonal movement field centers for 23 of the neurons we studied (1 neuron that began bursting only after movements had begun and 1 neuron that generated only a few bursts, all of which were determined to be outliers by our maximal burst lead identification algorithm, are not presented). Note that the distribution of polygons nearly spans the contraversive and downward halves of the portion of the oculomotor range we sampled. The majority of the area of 83% of the computed polygons was within the contraversive half of oculomotor space; the majority of the area of 87% of the polygons was within the lower half of oculomotor space. None of the neurons in this population were tuned for ipsiversive upward movements. Figure 5 presents a frequency histogram for this population of cMRF neurons of the 80% maximum burst lead values we observed [43.5 ± 5.4 (SE) ms].

TEMPORAL CORRELATIONS: BURST OFFSET AND SACCADE OFFSET. For each neuron we plotted, for all trials on which a burst was detected, the latency from the offset of the fixation LED (the initiation cue) to burst offset as a function of the latency from the offset of the fixation LED to the offset to the saccade. This permitted us to assess how tightly the time of cMRF burst offset was correlated with the time of movement offset. For the neuron presented in Fig. 6*A*, the latency to burst offset and the latency to movement offset were well correlated ($r = 0.814$); on average, the burst ended ~22 ms before the movement ended (Y-intercept = −21.5 ms; slope = 1.04). However, for the neuron analyzed in Fig. 6*B*, the latency to burst offset and the latency to movement offset were not as well correlated ($r = 0.234$). Across this population of neurons, the correlation between latency to movement offset and latency to burst offset varied from −0.886 to 0.814 ($r = 0.439 \pm 0.363$, SD; minimum $r^2 = 0.000$; maximum $r^2 = 0.785$; $r^2 = 0.319 \pm 0.239$, SD).

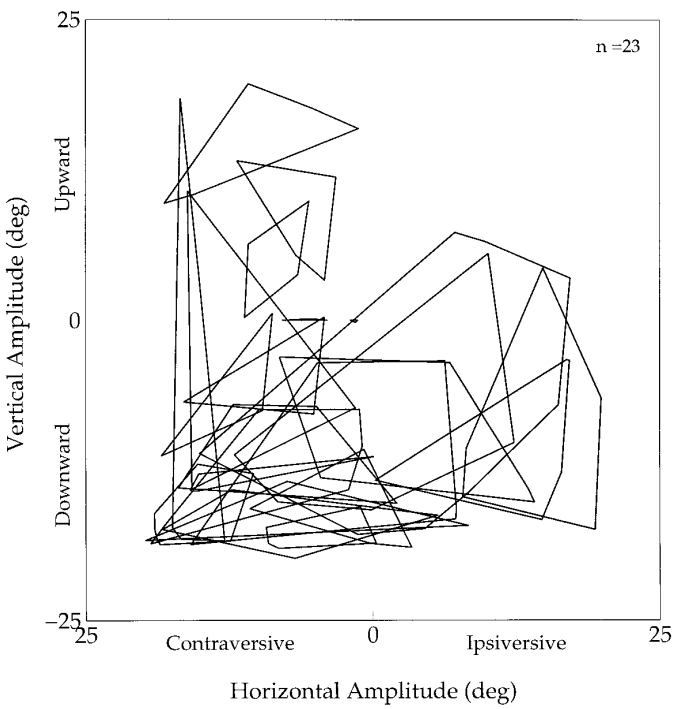

FIG. 4. Polygons representing movements associated with longest burst leads for all units generating presaccadic bursts during delayed saccade task. Each neuron is represented by the convex enclosure that encloses all movements from trials where burst lead was ≥80% of maximal burst lead. Variance in burst lead for movements in these polygons can be seen for 3 neurons in Fig. 3.

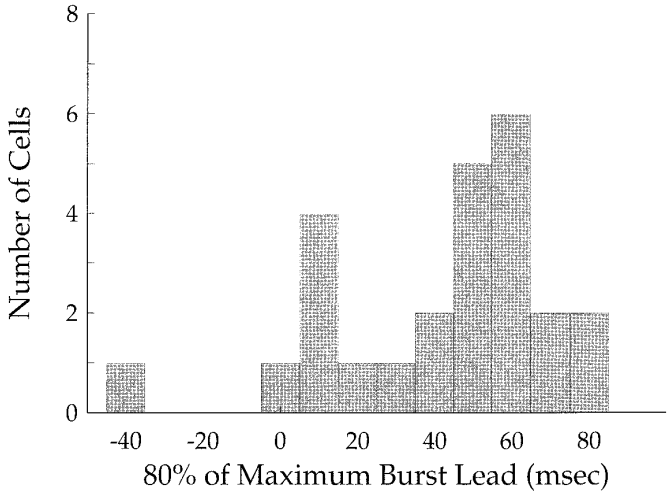

FIG. 5. Frequency distribution, for all neurons in our sample, of 80% of maximal burst lead. Mean of this distribution was 43.5 ± 5.4 (SE) ms.

Experiment 2: differential responses of cMRF neurons to targets and distractors

SINGLE-TRIAL DATA. Figure 7, *top*, plots the horizontal and vertical position of the eye, as well as the instantaneous firing rate of a single neuron as a function of time, during two trials of the cued saccade task. The four tick marks on the horizontal axes represent the times, successively, at which *1*) the eccentric LEDs were illuminated; *2*) the fixation LED changed color, identifying the saccadic goal; *3*) the fixation LED was extinguished, indicating that a saccade shifting gaze into alignment with the saccadic target within 350 ms would be reinforced; and *4*) the onset of the saccade. During both trials the upper eccentric LED was illuminated 20° to the left and 20° above the fixation LED (−20, 20), and the lower LED was illuminated 10° to the right and 10° below the fixation LED (10, −10). These locations were selected because on delayed saccade trials in which the single target was located at (−20, 20) the neuron was strongly active, but when the target was located at (10, −10) the neuron was inactive. Note that during both trials, the neuron began firing shortly after the eccentric LEDs were illuminated.

The trials in Fig. 7, *A* and *B* did, however, differ in one important respect: in Fig. 7*A* the fixation LED changed color from yellow to red, identifying the upper LED as the saccadic target. In Fig. 7*B* the fixation LED changed color from yellow to green, identifying the upper LED as an irrelevant distractor. Thus these trials differed visually only in the color of the fixation LED after the second tick mark. After the

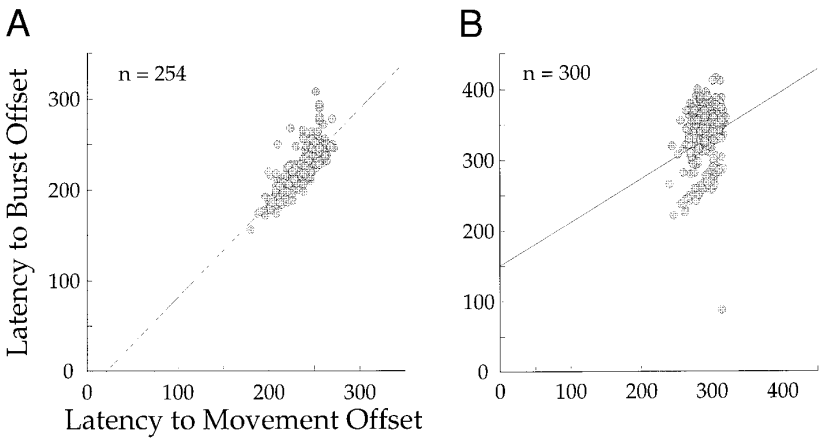

FIG. 6. Scatter plots of latency from fixation LED offset to burst offset as function of latency from fixation LED offset to movement offset for 2 neurons (*p070795* and *p0720952*, respectively). Values for best fit lines: slope, 1.04 (*A*), 0.62 (*B*); *Y*-intercept, −21.5 (*A*), 150.5 (*B*); associated *r*, 0.814 (*A*), 0.234 (*B*).

fixation LED turned red during the trial depicted in Fig. 7*A*, the instantaneous firing rate of the neuron increased and remained at this increased level until the neuron generated a high-frequency volley of action potentials just before and during the movement. In contrast, Fig. 7*B* shows that after the fixation LED turned green, the instantaneous firing rate of the neuron decreased, and the neuron remained relatively inactive during the movement.

Below each of the plots of instantaneous spike frequency in Fig. 7, *A* and *B*, the times of spike occurrence, during 10 additional reinforced trials with identically colored and positioned LEDs, are plotted. Note that the actual movements produced on these trials are not shown in this figure. The raster diagrams are split into three segments for these trials; each segment is temporally aligned with a distinct event in the trial. The *first column* of rasters is aligned with the time at which the eccentric LEDs were illuminated. The *second column* of rasters is aligned with the unpredictable offset of the fixation LED. The *third column* is aligned with movement onset. Complete rasters for these trials are not shown because each of the intervals from which these rasters were drawn varied randomly in length from trial to trial. It should also be noted that these visually identical trials were not presented in a block but have been extracted from the complete data base of trials during which the position of one eccentric LED was varied randomly.

The clear difference in firing rate between these two groups of visually similar trials (Fig. 7, *top*) indicates that the activity of the neuron after the fixation LED changed color was associated with the metrics of the upcoming saccade (and with the location of the saccadic target). This is because the only visual difference between the two sets of trials was the color to which the fixation LED changed. The possibility that the differential firing rates observed in these two groups of trials were correlated specifically with the color of the fixation LED can be largely excluded by examining error trials—those trials on which the animal shifted gaze into alignment with the LED specified as the irrelevant distractor. Two such error trials are plotted in Fig. 7, *bottom.* Although these trials were visually identical to the trials depicted above them, the movements made by the monkey were different. Notice that across both reinforced and error trials the activity level of the neuron was more tightly coupled with the movement the monkey generated than it was with the color to which the fixation LED changed.

Figure 8 plots the activity of a second neuron during single trials of the cued saccade task. Although this neuron began firing before the eccentric LEDs were illuminated, the firing rate was similar during both trials until after the fixation LED changed color. After the fixation LED turned green (Fig. 8*A*), the neuron maintained its firing rate and generated a small burst of action potentials immediately before the movement. In contrast, after the fixation LED turned red (Fig. 8*B*) the firing rate of the neuron decreased. However, the difference in activity between the two groups of trials (Fig. 8, *A* and *B*) was not as pronounced as it was for the neuron whose activity was depicted in Fig. 7. In the population of neurons we studied, the neuron presented in Fig. 7 showed the most dramatic difference in responses between trials on which the variable LED served as a target and trials on which that same LED served as an irrelevant distractor, whereas the neuron depicted in Fig. 8 was more typical.

SPATIAL TUNING OF TARGET AND DISTRACTOR RESPONSES. To examine the relationship between neuronal response and movement metrics, we plotted the mean firing rate of each neuron during the three selected intervals as a function of the horizontal and vertical amplitude of the movement made at the end of the trial. One set of these three-dimensional plots, for the neuron analyzed in Fig. 7, is presented in Fig. 9, *left.* Note that during the 200-ms interval beginning at the onset of the eccentric LEDs (Fig. 9, *top;* a time at which the animal could not know which of the two eccentric LEDs would later be identified as the saccadic goal), this neuron was weakly active on some trials. During the 200-ms interval ending at the offset of the fixation LED (Fig. 9, *middle*), however, the neuron was more active, particularly on trials where the monkey would later make large-amplitude gaze shifts up and to the left. Finally, during the 100-ms interval centered on movement onset (Fig. 9, *bottom*), the peak activity rate of the neuron increased dramatically, and, again, especially so for gaze shifts up and to the left.

To assess whether a distractor stimulus illuminated at these same locations was also associated with activation of this neuron, we plotted firing rate during our three intervals as a function of the horizontal and vertical position of the variable LED (Fig. 9, *right*) for all trials on which it served as a distractor. During all three of these intervals this neuron was essentially inactive, regardless of the position of the distractor LED in the upper hemifield. Most of the neurons

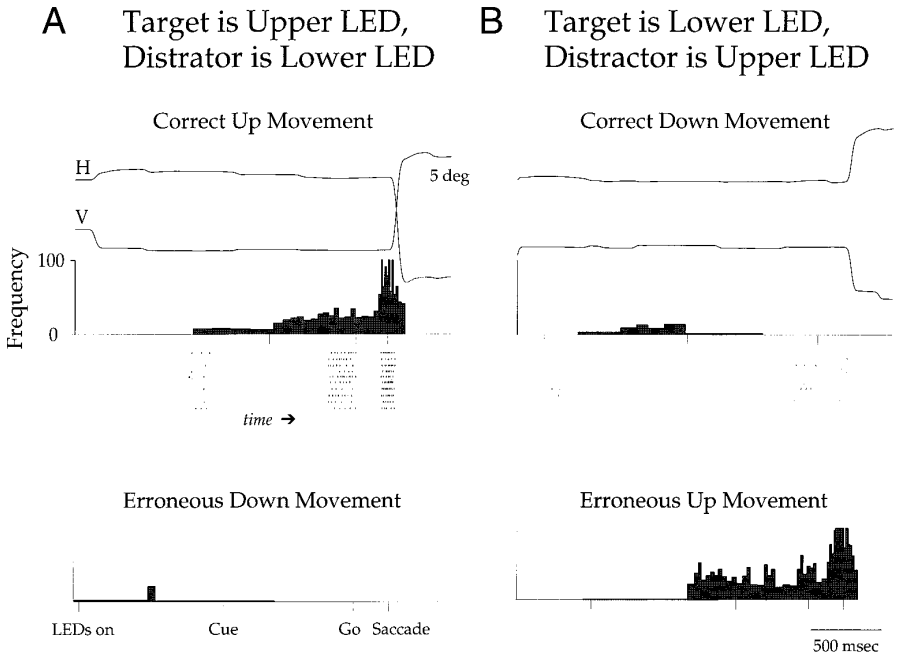

FIG. 7. Activity of single neuron (*p091595*) during single trials of cued saccade task. Horizontal and vertical coordinates, in deg of visual angle, of 2 eccentric LEDs were (−20, 20) and (10, −10). *A*: trials in which fixation LED turned red, specifying upper eccentric LED as target. *B*: trials in which fixation LED turned green, specifying lower eccentric LED as target. *Top*: horizontal and vertical eye position for single trial plotted as function of time above histogram of instantaneous firing frequency of neuron on that trial. The 4 tick marks below histogram indicate times, respectively, of onset of eccentric LEDs, color change of fixation LED, offset of fixation LED, and onset of saccade. Gray shaded rectangles: the 3 intervals during which activity was measured for further analyses. Raster segments, indicating time of spike occurrence, for 10 visually identical trials, are displayed within these rectangles. Average firing frequency during visual, cue, and movement intervals, respectively, for all trials: 6.4, 33.2, and 74.6 Hz (*A, top*); 1.4, 2.7, and 0.9 Hz (*B, top*). *Bottom*: histograms of instantaneous firing frequency are displayed for visually identical error trials during which monkey made an unreinforced saccade that aligned gaze with eccentric LED that was specified as distractor.

we studied did, however, show some activity that was coupled with the location of the visual distractor. In this sense, the neuron analyzed in Fig. 9 was atypical.

Figure 10 presents similar analyses for a second neuron, single-trial data for which was presented in Fig. 8. During the cue interval, the difference between the peak responses to targets and the peak responses to distractors was lower than it was for the neuron in Fig. 9. Thus during this interval an analysis of the firing rate of the neuron in Fig. 9 could distinguish between a target LED and a distractor LED more effectively than could a similar analysis of the firing rate of the neuron in Fig. 10.

We quantified the selectivity of each neuron for targets over distractors, during each interval, with the use of our selectivity ratio in which 0 indicates no selectivity for targets over distractors and 1 indicates perfect selectivity for targets. The selectivity scores for the neuron presented in Fig. 9 during the visual, cue, and movement intervals were −0.03, 0.83, and 0.88, respectively. Selectivity scores for the neuron presented in Fig. 10 were −0.04, 0.15, and 0.29. The firing rates of these two neurons were unselective during the visual interval, a time when the animal had insufficient information to discriminate targets from distractors.

The three histograms in Fig. 11 plot the distribution of

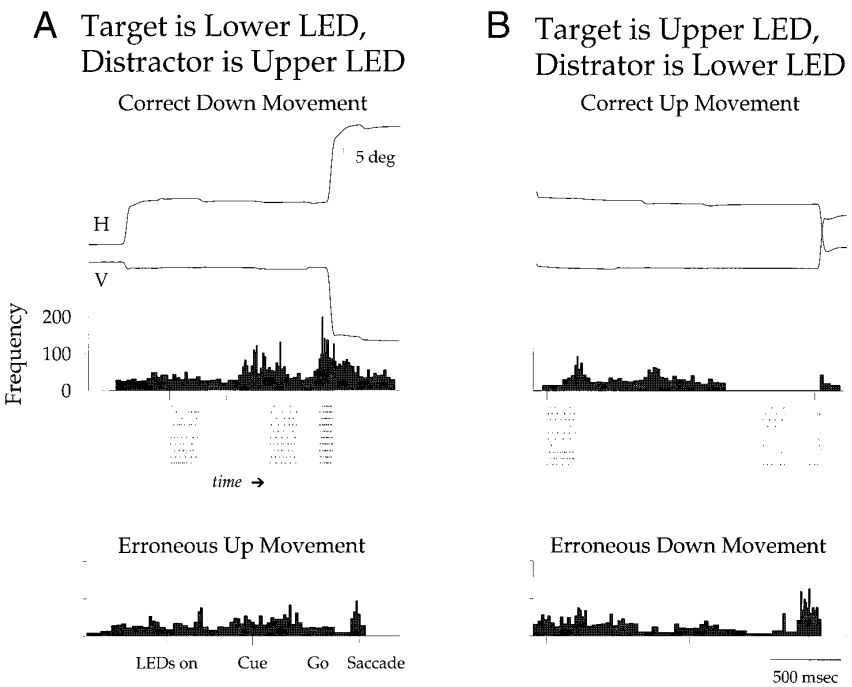

FIG. 8. Activity of neuron (*p0830952*) during single trials of cued saccade task during which coordinates of 2 eccentric LEDs were (16, −16) and (−10, 10). Plots are similar to those displayed in Fig. 7. Average firing frequency during visual, cue, and movement intervals, respectively: 25.9, 29.1, and 85.5 Hz (*A, top*); 25.5, 8.2, and 8.1 Hz (*B, top*).

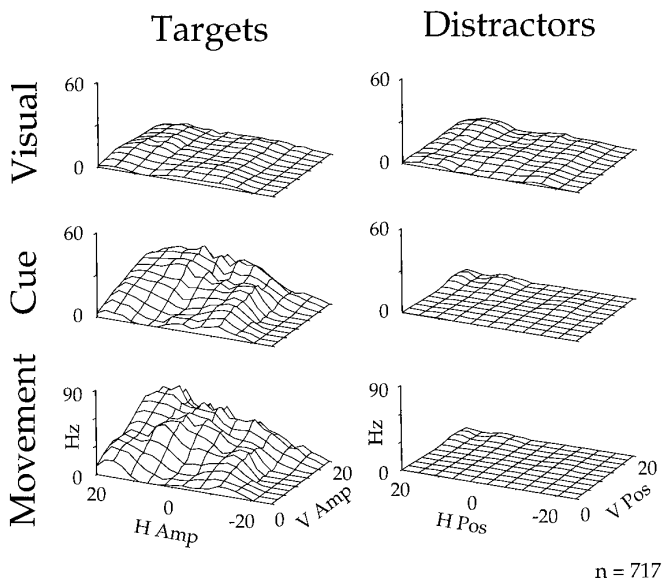

FIG. 9. Mean frequency of firing of single neuron (*p091595*) during visual, cue, and movement intervals (*rows*) of cued saccade task as function of horizontal and vertical amplitude of movement (*left*) and horizontal and vertical location of distractor (*right*). During trials used to compile plots on *left*, LED serving as distractor was fixed at location that yielded no spatially tuned increase of activity during any interval of delayed saccade task. During trials used to compile plots on *right*, LED serving as target was fixed at this location. When presented to animal, these 2 sets of trials were randomly interleaved. For all plots, data were averaged into 2.5 × 2.5° bins and represented as a smoothed surface (Axum). Plotted area was truncated to avoid display of edge effects introduced by smoothing algorithm. Peak of target surfaces in visual, cue, and movement intervals: 8, 31, and 62 Hz, respectively. Respective peaks for distractor plots: 8, 4, and 4 Hz. Note change in frequency scale in plots for movement interval.

selectivity index values for the 26 neurons we studied during each of the three intervals. The mean selectivities during the visual, cue, and movement intervals were -0.03 ± 0.03 (SE), 0.15 ± 0.06 (SE), and 0.59 ± 0.05 (SE), respectively. The means of the distributions in the cue and movement intervals were significantly higher than zero (single-sample *t*-test: $P < 0.05$, $P < 0.001$, respectively). The mean firing rates for the maximum target bins, which are not explicitly communicated by the selectivity indexes, were 40.6 ± 28.8 (SD) Hz, 53.8 ± 38.5 (SD) Hz, and 156.0 ± 78.5 (SD) Hz, respectively.

Anatomy/histology

Figure 12 is a schematic representation of camera lucida reconstructions of four lesions placed at recording sites where neurons of the type described in this report were encountered. All four lesion sites (indicated by ∗) were located in the cMRF region (as defined by Cohen et al. 1985; Waitzman et al. 1996), lateral to the oculomotor nucleus and just lateral and dorsal to the red nucleus.

DISCUSSION

Stimulation of either the frontal eye fields or the SC produces eye movements with the metrical and dynamic properties of natural saccades (Bruce et al. 1985; Robinson 1972). However, if both of these structures are lesioned, saccades cannot be generated (Schiller et al. 1980). These and other results have led some investigators to propose that the colliculus and frontal eye fields serve as final common pathways for the execution of saccadic eye movements (Bruce and Goldberg 1985) that are interposed between high-level movement planning systems and brain stem movement execution centers. This hierarchical view often implicitly assumes that brain stem saccade-related neurons participate exclusively in signal processing that occurs after collicular and/or frontal eye field neurons issue a neural command to initiate a movement.

Two major classes of hypotheses about the function of the SRBNs of the cMRF have been proposed, both of which are consistent with this hierarchical view of the saccadic system. In the first class of hypotheses, cMRF neurons have been proposed to participate in the transmission of saccade-related signals from the SC to horizontally tuned pontine MLBNs (Sparks and Mays 1990; Waitzman et al. 1996). Anatomic support for this proposal includes observations that the cMRF receives afferent projections from the intermediate and deep layers of the ipsilateral SC (Cohen and Büttner-Ennever 1984; Moschovakis et al. 1988) and sends an efferent projection to the contralateral pontine reticular formation (Büttner-Ennever and Büttner 1988; Edwards 1975). In the second class of hypotheses, the cMRF has been proposed to provide the SC with feedback from the pontine MLBNs for use in the dynamic control of ongoing saccades (Waitzman et al. 1996). This second class of hypotheses is supported by reports that cMRF neurons project bilaterally to the deep and intermediate layers of the SC (Cohen and Büttner-Ennever 1984; Moschovakis et al. 1988) and receive ascending projections from the pontine reticular formation (Büttner-Ennever and Büttner 1988; Gray-

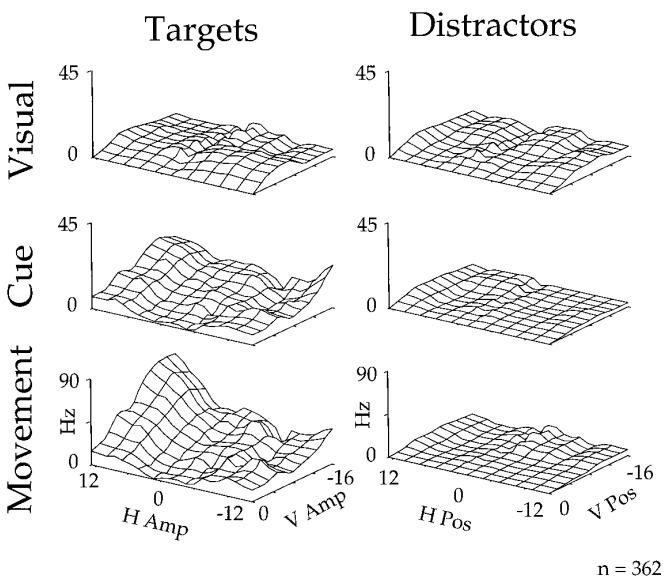

FIG. 10. Mean frequency of firing of single neuron (*p0830952*) during visual, cue, and movement intervals (*rows*) of cued saccade task as function of horizontal and vertical amplitude of movement (*left*) and horizontal and vertical location of distractor (*right*). Plots are compiled and displayed as in Fig. 9. Peaks of surfaces in target plots during visual, cue, and movement intervals: 10, 24, and 83 Hz, respectively. Peaks of surfaces in distractor plots for same intervals: 11, 7, and 12 Hz. Activity of this neuron during single trials of cued saccade task is presented in Fig. 8. Note change in frequency scale in plots for movement interval.

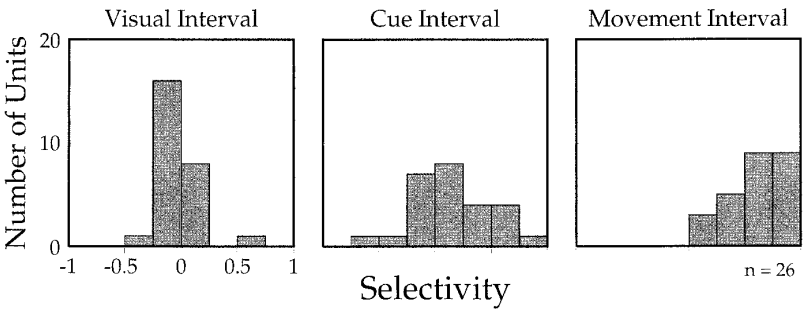

FIG. 11. Frequency distributions, for population of 26 neurons studied, of selectivities [(peak activity for targets − peak activity for distractors)/(peak activity for targets + peak activity for distractors)] during visual, cue, and movement intervals. Mean selectivities during cue and movement intervals were significantly >0.0 (single-sample *t*-test, cue interval: $P < 0.05$; movement interval: $P < 0.001$).

biel 1977). Both classes of hypotheses propose that cMRF neurons receive command signals ultimately originating in the colliculus and, on the basis of these signals, participate in the execution of saccades that have already been initiated (see also Moschovakis et al. 1988, who propose that cMRF neurons form part of a tectal-tegmental-tectal feedback loop specifying motor error). To examine these hypotheses, we analyzed the activity of cMRF saccade-related neurons while animals performed oculomotor tasks.

Spatial tuning

Current evidence indicates that a desired movement vector is first specified by an active population of collicular neurons and then decomposed into the independent horizontal and vertical subcomponents represented by the firing rates of horizontally and vertically tuned MLBN populations (Fuchs et al. 1985; Sparks and Mays 1990). The hypothesis that cMRF neurons are involved in the transmission of saccade-related signals from the SC to the MLBNs suggests that this transformation may be partially or completely accomplished at the level of the cMRF. The hypothesis that the cMRF is involved in the feedback of pontine MLBN signals to the colliculus makes a similar prediction, because the inverse transformations are required.

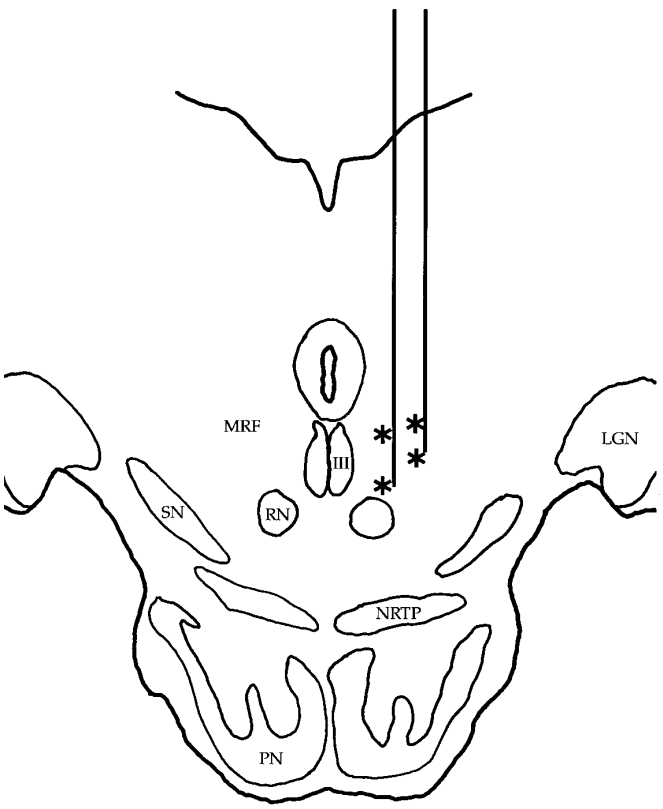

FIG. 12. Schematic representation of camera lucida drawings of 4 lesions (*) placed at sites where single units with properties of cMRF neurons were recorded. III, oculomotor nucleus; LGN, lateral geniculate nucleus; MRF, mesencephalic reticular formation; NRTP, nucleus reticularis tegmenti pontis; PN, pontine nuclei; RN, red nucleus; SN, substantia nigra.

Previous studies of the cMRF have supplied evidence that is consistent with either of these hypotheses: stimulation of the cMRF region has been shown to produce saccades that are primarily contraversive (Cohen et al. 1985), and global averages of cMRF population activity have been reported to covary with the amplitude of contraversive saccades (Waitzman et al. 1996). These observations have led, specifically, to the proposal that cMRF SRBNs carry, and supply the horizontal MLBNs with, a signal specifying the horizontal component of impending or ongoing saccades (Sparks and Mays 1990). The results of the present study, however, are less supportive of the proposal that cMRF neurons carry a signal that specifies horizontal saccadic amplitude explicitly. We found that burst frequency, burst duration, and burst lead varied systematically as a function of both horizontal and vertical movement amplitude for most of the neurons we examined. Although it is possible that a global average of the activity of this population covaries with the amplitude of contraversive saccades, there is no indication in our data that neurons of the cMRF uniquely code the horizontal amplitude of impending or ongoing saccades.

Burst lead in cMRF neurons

If initiation-related bursting activity in the cMRF is generated by initiation-related bursting activity in the SC, then the onset of bursting activity in the population of collicular neurons should precede the onset of bursting activity in the population of cMRF neurons. Previous investigators have reported that, on average, cMRF neurons begin bursting ~11–18 ms before movement onset (Moschovakis et al. 1988; Waitzman et al. 1996). Collicular SRBNs, in contrast, have been reported to begin bursting ~18–20 ms before the onset of movements into the center of their movement fields (Sparks 1978; Sparks and Mays 1980; Sparks et al. 1976).

However, it is difficult to compare estimates of burst lead produced by different investigators. This difficulty arises from *1*) the use of different methods for estimating burst lead in individual neurons; *2*) the observation that in many populations burst lead varies systematically with movement

metrics (Kaneko et al. 1981; Sparks et al. 1976); and *3*) the fact that a common method for determining the burst lead of a neuronal population, calculating the mean burst lead for all movements into the movement field center of each neuron, does not accurately estimate the earliest time at which a neuronal population carries information about the onset time of a movement and depends heavily on the accuracy and methodology for identifying the movement field center.

In an effort to estimate when, on average, activity in the population of 25 neurons we studied could reliably signal movement onset, we first determined the longest reliable burst lead produced by each neuron. We then defined the movement field center of each neuron as the range of movement amplitudes and directions associated with burst leads whose duration was $\geq$80% of this maximum. For the neurons in our sample, these ranges of movement amplitudes and directions nearly span the contraversive hemisphere. Thus, in principle, any contraversive movement would fall within the movement field center of at least one of the neurons in our sample. On average, 38% of the movements into the movement field center of each neuron were associated with burst leads within 80% of the maximum burst lead for that neuron. Thus, before 38% of contraversive saccades, regardless of their metrics, at least one neuron in our sample would generate a burst whose onset led movement onset by $\geq$80% of the maximum burst lead produced by that neuron. If we therefore assume that the cMRF contains $\geq$3 times the number of neurons we sampled, that these neurons have characteristics similar to those in our sample, and that the trial-to-trial variance in burst lead of these neurons are relatively independent, then we can suggest that bursting activity (defined as an increase in firing rate 4 SD above baseline) is first present in the cMRF at least as long as 80% of the maximum burst leads generated by our sample of neurons. Thus, on the basis of an analysis of the bilateral population of cMRF neurons, it might be possible to predict that a movement will be impending $\geq$43.5 ms before that movement occurs.

It is important to note that we used a relatively stringent statistical method to define the time of burst onset. Relaxing our definition of burst onset (for instance, using a longer baseline interval, a lower burst frequency threshold, or a less conservative definition of maximal burst lead) would have led to a longer estimate of the burst lead for this population of neurons. Moreover, our estimate was based on 80% of the maximal burst lead generated by the neurons we studied, because the movement field centers based on this threshold nearly spanned the contraversive hemisphere. If we had sampled more neurons, the same area may have been spanned by movement field centers based on a higher threshold, again leading to a longer estimate of the population burst lead.

cMRF activity appropriate for the dynamic control of saccades

It has been proposed that high-frequency bursts of activity produced by cMRF saccade-related neurons are involved in the dynamic control of saccades as part of a colliculopontocollicular feedback loop (Waitzman et al. 1996). In the data presented here, however, there is no consistent temporal relationship between burst offset and movement offset across this population of cMRF neurons.

cMRF activity appropriate for processes that precede movement initiation

Some saccade-related neurons in the SC have been shown to generate a low-frequency prelude of activity before their high-frequency burst (Sparks 1978; Wurtz and Goldberg 1972). The frequency of these preludes in individual neurons has been shown to be related to the metrics of upcoming movements, and, to a lesser degree, to the location of visual distractors (Glimcher and Sparks 1992). These data indicate that the metrics of upcoming movements might be predicted from the activity of a population of collicular prelude bursting neurons long before neural processes initiating those movements have begun.

Previous investigators have reported that, like collicular prelude burst neurons, some cMRF neurons generate low-frequency preludes of activity before their high-frequency bursts of activity (Waitzman 1982). Our examination of cMRF neurons revealed that this prelude of activity carries information related to both the metrics of future saccades and, to a lesser extent, the location of visual distractors, during an interval when saccade initiating processes cannot have begun. One possibility is that collicular prelude burst neurons serve as the source of this signal. This hypothesis might suggest that the selectivity of cMRF neurons for targets versus distractors (see METHODS) during the cue interval would be greater or equal to that of prelude burst neurons. However, the selectivity of our sample population during this interval (cue interval selectivity = 0.14) was considerably lower than that reported for collicular prelude burst neurons (cue interval selectivity = 0.3) examined with similar tasks (Glimcher and Sparks 1992). This suggests either that collicular prelude burst neurons are not the source of cMRF prelude activity or that signals carried by collicular preludes become less reliable indicators of future movement metrics before reaching the cMRF.

Conclusions

SRBNs in the cMRF generate a high-frequency burst of action potentials before saccades that is sometimes preceded by a prelude of low-frequency activity. We found that *1*) burst duration, mean burst frequency, and burst lead all varied systematically with horizontal and vertical movement amplitude; *2*) bursting activity may be present in the cMRF population $>$40 ms before the onset of saccades; *3*) low-frequency prelude responses in the cMRF carry a signal appropriate for premovement processes; and *4*) this premovement signal appears not to distinguish between future movement metrics and the location of visual distractors as strongly as does the population of collicular prelude burst neurons. Taken together, these results raise the possibility that bursting neurons in the cMRF may be involved in signal processing that precedes the initiation of saccadic eye movements by the SC. Further, the hypothesis that cMRF neuronal activity exclusively encodes the horizontal component of impending or ongoing saccades is not supported by these data.

The authors thank Dr. Michael Platt and an anonymous reviewer for helpful comments on the manuscript, M. Brown for assisting in some of the experiments, J. Mones for help with the histology, and S. Corathers and H. Tamm for technical support. We also thank Dr. David L. Sparks and K. Pearson for the use of data analysis software.

This work was supported by National Institutes of Health Grants EY-10536 (to P. W. Glimcher) and F31 MH-11359 (to A. Handel).

Address for reprint requests: A. Handel, Center for Neural Science, New York University, 4 Washington Place, Room 809, New York, NY 10003.

Received 25 October 1996; accepted in final form 17 March 1997.

REFERENCES

BRUCE, C. J. AND GOLDBERG, M. E. Primate frontal eye fields. I. Single neurons discharging before saccades. *J. Neurophysiol.* 53: 603–635, 1985.

BRUCE, C. J., GOLDBERG, M. E., BUSHNELL, C., AND STANTON, G. B. Primate frontal eye fields. II. Physiological and anatomical correlates of electrically evoked eye movements. *J. Neurophysiol.* 54: 714–734, 1985.

BÜTTNER-ENNEVER, J. A. AND BÜTTNER, U. The reticular formation. In: *Neuroanatomy of the Oculomotor System*, edited by J. A. Büttner-Ennever. Amsterdam: Elsevier, 1988, p. 119–176.

CHIMOTO, S., IWAMOTO, Y., SHIMAZU, H., AND YOSHIDA, K. Monosynaptic activation of medium-lead burst neurons from the superior colliculus in the alert cat. *J. Neurophysiol.* 75: 2658–2661, 1996.

COHEN, B. AND BÜTTNER-ENNEVER, J. A. Projections from the superior colliculus to a region of the central mesencephalic reticular formation (cMRF) associated with horizontal saccadic-eye movements. *Exp. Brain Res.* 57: 167–176, 1984.

COHEN, B., MATSUO, V., FRADIN, J., AND RAPHAN, T. Horizontal saccades induced by stimulation of the central mesencephalic reticular formation. *Exp. Brain Res.* 57: 605–616, 1985.

EDWARDS, S. B. Autoradiographic studies of the projections of the midbrain reticular formation: descending projections of nucleus cuneiformis. *J. Comp. Neurol.* 161: 341–356, 1975.

FUCHS, A. F., KANEKO, C.R.S., AND SCUDDER, C. A. Brainstem control of saccadic eye movements. *Annu. Rev. Neurosci.* 8: 307–337, 1985.

FUCHS, A. F. AND LUSCHEI, E. S. Firing patterns of abducens neurons of alert monkeys in relationship to horizontal eye movement. *J. Neurophysiol.* 33: 382–392, 1970.

FUCHS, A. F. AND ROBINSON, D. A. A method for measuring horizontal and vertical eye movement chronically in the monkey. *J. Appl. Physiol.* 21: 1068–1070, 1966.

GLIMCHER, P. W. AND SPARKS, D. L. Movement selection in advance of action in the superior colliculus. *Nature Lond.* 355: 542–545, 1992.

GRAYBIEL, A. M. Direct and indirect preoculomotor pathways of the brainstem: an autoradiographic study of the pontine reticular formation in the cat. *J. Comp. Neurol.* 175: 37–78, 1977.

JUDGE, S. J., RICHMOND, B. J., AND CHU, F. C. Implantation of magnetic search coils for measurement of eye position: an improved method. *Vision Res.* 20: 535–538, 1980.

KANEKO, C.R.S., EVINGER, C., AND FUCHS, A. F. Role of cat pontine burst neurons in generation of saccadic eye movements. *J. Neurophysiol.* 46: 387–408, 1981.

LEE, C., ROHRER, W. H., AND SPARKS, D. L. Population coding of saccadic eye movements by neurons in the superior colliculus. *Nature Lond.* 332: 357–360, 1988.

MOSCHOVAKIS, A. K. AND HIGHSTEIN, S. M. The anatomy and physiology of primate neurons that control rapid eye movements. *Annu. Rev. Neurosci.* 17: 465–488, 1994.

MOSCHOVAKIS, A. K., KARABELAS, A. B., AND HIGHSTEIN, S. M. Structure-function relationships in the primate superior colliculus. II. Morphological identity of presaccadic neurons. *J. Neurophysiol.* 60: 232–262, 1988.

RAYBOURN, M. S. AND KELLER, E. L. Colliculoreticular organization in primate oculomotor system. *J. Neurophysiol.* 40: 861–878, 1977.

ROBINSON, D. A. Oculomotor unit behavior in the monkey. *J. Neurophysiol.* 33: 393–404, 1970.

ROBINSON, D. A. Eye movements evoked by collicular stimulation in the alert monkey. *Vision Res.* 12: 1795–1808, 1972.

SCHILLER, P. The discharge characteristics of single units in the oculomotor and abducens nuclei of the unanesthetized monkey. *Exp. Brain Res.* 10: 347–362, 1970.

SCHILLER, P. H., TRUE, S. D., AND CONWAY, J. L. Deficits in eye movements following frontal eye-field and superior colliculus ablations. *J. Neurophysiol.* 44: 1175–1189, 1980.

SPARKS, D. L. Functional properties of neurons in the monkey superior colliculus: coupling of neuronal activity and saccade onset. *Brain Res.* 156: 1–16, 1978.

SPARKS, D. L., HOLLAND, R., AND GUTHRIE, B. L. Size and distribution of movement fields in the monkey superior colliculus. *Brain Res.* 113: 21–34, 1976.

SPARKS, D. L. AND MAYS, L. E. Movement fields of saccade-related burst neurons in the monkey superior colliculus. *Brain Res.* 190: 39–50, 1980.

SPARKS, D. L. AND MAYS, L. E. Signal transformations required for the generation of saccadic eye movements. *Annu. Rev. Neurosci.* 13: 309–336, 1990.

WAITZMAN, D. M. *Burst Neurons in the Mesencephalic Reticular Formation (MRF) of the Rhesus Monkey Associated With Saccadic Eye Movements* (PhD thesis). New York: City Univ. of New York, 1982.

WAITZMAN, D. M., SILAKOV, V. L., AND COHEN, B. Central mesencephalic reticular formation (cMRF) neurons discharging before and during eye movements. *J. Neurophysiol.* 75: 1546–1572, 1996.

WURTZ, R. H. AND GOLDBERG, M. E. Activity of superior colliculus in behaving monkey. III. Cells discharging before eye movements. *J. Neurophysiol.* 35: 575–586, 1972.